NJC

New Journal of Chemistry

A journal for new directions in chemistry

Accepted Manuscript

This article can be cited before page numbers have been issued, to do this please use: A. Kharma, A. Misak, M. Grman, V. Brezova, L. Kurakova, P. Barath, C. Jacob, M. Chovanec, K. Ondrias and E. Domínguez-Álvarez, *New J. Chem.*, 2019, DOI: 10.1039/C9NJ02245G.

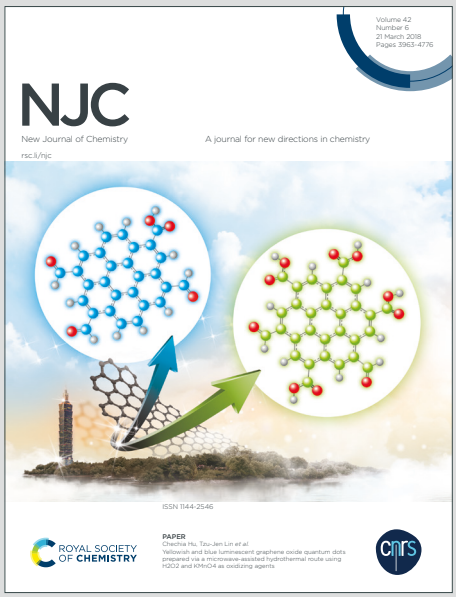

This is an Accepted Manuscript, which has been through the Royal Society of Chemistry peer review process and has been accepted for publication.

Accepted Manuscripts are published online shortly after acceptance, before technical editing, formatting and proof reading. Using this free service, authors can make their results available to the community, in citable form, before we publish the edited article. We will replace this Accepted Manuscript with the edited and formatted Advance Article as soon as it is available.

You can find more information about Accepted Manuscripts in the Information for Authors.

Please note that technical editing may introduce minor changes to the text and/or graphics, which may alter content. The journal's standard Terms & Conditions and the Ethical guidelines still apply. In no event shall the Royal Society of Chemistry be held responsible for any errors or omissions in this Accepted Manuscript or any consequences arising from the use of any information it contains.

View Article Online
DOI: 10.1039/C9NJ02245G

ARTICLE

Release of Reactive Selenium Species from phthalic selenoanhydride in the presence of hydrogen sulfide and glutathione with implications for cancer research

Received 00th January 20xx,
Accepted 00th January 20xx

DOI: 10.1039/x0xx00000x

Ammar Kharma[a,b], Anton Misak[a], Marian Grman[a], Vlasta Brezova[c], Lucia Kurakova[d], Peter Baráth[e], Claus Jacob[b], Miroslav Chovanec[f], Karol Ondrias[a] and Enrique Domínguez-Álvarez*[g]

The last decade has witnessed a renewed interest in selenium (Se) as an element able to prevent a range of illnesses in humans, mainly through supplementation. However, such supplementation relies on species such as sodium selenite or selenomethionine that proved to have limited solubility and bioavailability, thus leading to a limited activity. To overcome this limitation, other selenium species need to be explored, as the phthalic selenoanhydride (R-Se), which is soluble in physiological media. R-Se releases various Reactive Selenium Species (RSeS), including hydrogen selenide (H_2Se), that can interact with cellular components, such as glutathione (GSH) and hydrogen sulfide (H_2S). This interplay between R-Se and the intracellular components provides a sophisticated biochemical release mechanism that could be behind the noteworthy biological activities observed for this compound. In order to investigate the interactions of phthalic chalcogen anhydrides with H_2S or GSH, we have employed UV-VIS spectrophotometry, electron spin resonance spectroscopy (ESR) and plasmid DNA (pDNA) cleavage assay. We found that apart from R-Se, the other analogues do not have ability to scavenge the $^{\bullet}$cPTIO radical or to cleave pDNA on their own. In contrast, the scavenging potency of $^{\bullet}$cPTIO radical and of $O_2^{\bullet-}$ radical exerted by R-Se and of its sulfur analogue (R-S) significantly increased when they were evaluated in presence of H_2S. However, GSH only changed the radical scavenging activity of R-Se. These new discoveries may explain some of the biological activities associated with this class of compounds and opens a new approach to ascertain the possible mechanisms underlying their biological actions.

Introduction

Selenium (Se) is an essential element for human health and its deficiency causes severe disorders, such as Keshan or Kashin-Beck diseases, which are endemic of farming self-sufficient regions with low levels of Se in the soil.[1,2] Both Se-containing compounds and the Se atom present in the active sites of 25 mammalian selenoproteins identified so far, participate in key cellular and physiological processes, as well as diseases such as cancer, inflammation, immunity, type 2 diabetes or liver diseases.[3-8] However, the molecular mechanism of action is not fully understood yet for some of these selenoproteins.

During recent years, Se-compounds have gained substantial interest as H_2Se donors, as potential anti-cancer agents or as selenocompounds with potential use in selenium supplementation.[8-11] Among other effects of Se-compounds related to cancer, they could induce apoptosis in cancer cells through the production of Reactive Oxygen Species (ROS) and thus inducing oxidative stress (OS).[12,13] Furthermore, certain Se-compounds can damage DNA. Then, they may not protect against cancer and other chronic diseases, and can even cause or enhance some types of cancer. These facts indicate that Se may exert a broad pattern of toxic effects. [14,15] The exact mechanisms underlying the beneficial and toxic effects of the Se-compounds are not fully understood yet and they are still under intensive investigation, due to the interest of the potential applications of this dual behaviour: these pro-oxidant/antioxidant Se-compounds could act as novel cellular redox modulators.

In this context, the accessibility and reactivity of the selenols (mainly deprotonated at biological pH values) and selenol-derived compounds, such as *Se*-methyl selenocysteine and diselenides,[16-19] may be behind the reported chemopreventive activity of different Se-containing compounds, which has been reviewed extensively by numerous authors.[11,20-25] Several

[a] Institute of Clinical and Translational Research, Biomedical Research Centre, University Science Park for Medicine, Slovak Academy of Sciences, Dúbravská cesta 9, 845 05 Bratislava, Slovak Republic.
[b] Division of Bioorganic Chemistry, School of Pharmacy, Saarland University, Campus B2 1, D-66123 Saarbruecken, Germany.
[c] Faculty of Chemical and Food Technology, Slovak University of Technology, Radlinskeho 9, 812 37 Bratislava, Slovak Republic.
[d] Department of Pharmacology and Toxicology, Faculty of Pharmacy, Comenius University, Ulica Odbojárov 10, 832 32 Bratislava, Slovak Republic.
[e] Institute of Chemistry, Slovak Academy of Sciences, Dúbravská cesta 9, 845 38 Bratislava, Slovakia.
[f] Cancer Research Institute, Biomedical Research Centre, University Science Park for Medicine, Slovak Academy of Sciences, Dúbravská cesta 9, 845 05 Bratislava, Slovak Republic.
[g] Instituto de Química Orgánica General, Consejo Superior de Investigaciones Científicas (IQOG, CSIC), Juan de la Cierva 3, 28006 Madrid, Spain.
Electronic Supplementary Information (ESI) available: [details of any supplementary information available should be included here]. See DOI: 10.1039/x0xx00000x

View Article Online DOI: 10.1039/C9NJ02345C

mechanisms have been proposed to explain the chemopreventive activity, such as the direct scavenging of free radicals,[26,27] the amelioration of the toxic effects of anticancer drugs,[28] the glutathione peroxidase (GPx)-like activity,[29,30] toxic elements such as arsenic by protecting PC12 cells from arsenic induced oxidative stress [31] or radiotherapy;[32] the modulation of the intracellular redox homeostasis[33] and of the protein kinases.[34]

In the last twenty years, H_2S ($H_2S/HS^-/S^{2-}$) has been emerging as a new gaseous signalling molecule besides nitric oxide ($^{\bullet}NO$) and carbon monoxide (CO). H_2S is produced endogenously in almost all mammalian cells and affects many physiological and pathological processes. [35-37] H_2S has mostly beneficial effects under conditions of oxidative stress by reacting with reactive oxygen and nitrogen species. [38-42] It has both the pro- and anti-cancer effects depending on the cell type, concentration and interaction with other cellular molecules. [43-45] Glutathione (GSH) is another intracellular natural antioxidant, which has many biological roles including modulation of cellular redox homeostasis and protection against reactive oxygen and nitrogen species.[46,47] As it has been determined in a previous work, sodium selenite (Na_2SeO_3) and selenium tetrachloride ($SeCl_4$) have ability to interact separately with GSH and H_2S. This fact could be behind their biological effects.[48] However, as mentioned above, sodium selenite can have reduced bioavailability and exert toxic effects. [14,15] Thus, it is desirable to move towards novel Se-containing compounds that retain this observed ability to interact with relevant sulfur compounds (herein, GSH and H_2S), and, at the same time, show a reduced toxicity in comparison with sodium selenite. This would improve the applicability of these new selenium-based redox modulators, and simultaneously, open a new approach in Se-supplementation, by finding of redox-active derivatives with less toxicity.

In this context, our previous data showed promising chemopreventive, antiproliferative, cytotoxic, free radical scavenging, pro-apoptotic and multidrug-resistance (MDR) reversing activity of phthalic selenoanhydride (R-Se, Figure 1), the Se-analogue of phthalic-anhydride.[49-52] Probably, these reported biological activities are directly related to the Se atom, as no relevant biological effects were displayed by its oxygen analogue, the phthalic anhydride (R-O).[51] A hypothesis which may explain the amazing biological properties of R-Se draws the attention to the lability of the CO-Se chemical bond.[49] This lability suggests the interesting possibility that R-Se behaves in the organism as a prodrug: It enables the internalization of the compound in the cells, and once inside, it can release selenium slowly inside the cell, in form of H_2Se, of other uncharged Se-species as nanoparticles of selenium or of charged Se-anions able to interact swiftly with cellular components.[49,51] Due to their particular chemical affinity towards thiol-containing agents, such as hydrogen sulfide (H_2S) or glutathione (GSH), and with the enzymes and proteins which are components of the cell thiolstat, such reactivity may initiate pronounced biological responses. In this way, R-Se could result to be a very simple, elegant and straightforward method to transport selenium inside the cells, and at the same time, it would enable its release in an "activated" form as one of the Reactive Selenium Species, ready to exert immediately a wide variety of biological effects. Besides, these compounds have proved in previous studies that can exert a selective action for being less toxic in non-tumour cells than in cancer cells.[49,51] Thus, they could be used as safer redox modulators.

Herein, we have studied further the possible mechanism(s) underlying these initial promising biological activities of R-Se, and we will ascertain if these hypothesized interactions with H_2S and GSH take effectively place. Activities of the R-O and phthalic thioanhydride (R-S) were examined in parallel for comparison. Since H_2S and GSH interact with several biologically active molecules modulating their activities.[42,46-48,53] Interactions of H_2S and GSH with these three phthalic anhydride derivatives and their molecular consequences were also analysed; expecting that in these instances, the R-Se would be the most reactive one thanks to its higher expected reactivity. The reduction of the $^{\bullet}$cPTIO and superoxide ($O^{2\bullet-}$) radicals, and plasmid DNA (pDNA) cleavage assay were employed to monitor these consequences. We show that only R-Se displays any significant biological activity on its own. This activity augmented considerably when tested in combination with H_2S or GSH. In contrast, GSH showed no impact over the activities of R-S or of R-O, whilst H_2S was efficient to some extent in this context. Hence, products of the H_2S or GSH interaction with R-Se and R-S show free radical scavenging properties and appear to cleave pDNA, potentially explaining some of their biological activities.

Results and discussion

To unveil the possible mechanisms underlying the reported activities of R-Se against cancer, we have designed different experiments with R-Se, R-S and R-O, as mass spectrometry (ESI-MS), spectrophotometrically-monitored radical scavenging and electron paramagnetic resonance (EPR); in an attempt to ascertain how this promising Se-containing compound can interact with different cellular redox targets.

Chemistry

In the present work, we have evaluated three chalcogen phthalic anhydrides, as shown in Figure 1: the phthalic selenoanhydride (X=Se → R-Se), the phthalic thioanhydride (X=S → R-S) and the phthalic anhydride (X=O → R-O), as well as phthalic acid (R-OH). R-O and R-OH were commercially available, whereas R-Se and R-S were synthesized following an adaption of the procedure previously described for the synthesis of R-Se (Figure 1). [49]

In brief words, elemental selenium or sulfur are reduced with lithium aluminium hydride, and the *in situ* formed hydrogen chalcogenide attacks the phthaloyl chloride to form a reactive intermediate. Sulphuric acid is added to form the desired final R-Se or R-S. Compounds were isolated in the form of stable solids, whose purity was assessed through NMR and LC-MS.

View Article Online
DOI: 10.1039/C9NJ02415C

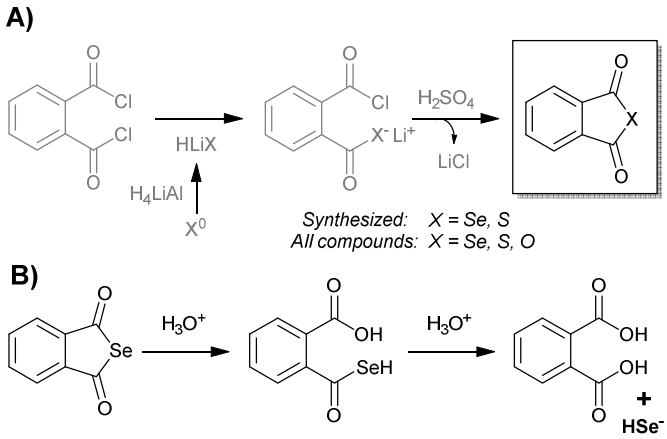

Figure 1. A). Chemical structure of the chalcogen derivatives of the phthalic anhydride. X= Se→ R-Se; S→ R-S; O→ R-O. Synthetic procedure for R-Se and R-S. B) Hypothesized reactions that would lead to the release of hydrogen selenide (H_2Se) from R-Se in the physiological media.

ESI-MS

R-Se showed a complex pattern of fragmentation (Figure 2) in ESI-MS (electrospray ionization mass spectrometry) spectrum taken in a 50% methanol/H_2O solution (Figure 3). The possible fragments corresponding with the main peaks observed in the ESI are suggested in Figure 2.

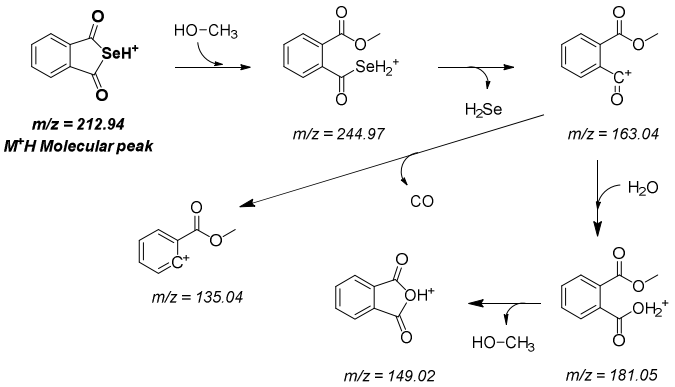

Figure 2: Hypothesized fragmentation pattern for protonated R-Se in ESI-MS.

The M^+H molecular peak of the R-Se is easily recognisable thanks to the characteristic isotopic pattern of the Se-containing fragments, and the remaining peaks of low m/z can be assigned to specific fragments (Figure 2). Briefly, the protonated molecular peak (*m/z* = 212.94487) is attacked by methanol to generate the fragment with *m/z* = 244.97104 (also with the characteristic isotopic pattern of Se). This fragment loses a molecule of hydrogen selenide, leading to the *m/z* =163.03906, which can suffer an additional fragmentation (release of CO, *m/z* = 135.04408) or can incorporate a molecule of water to later generate the protonated R-O (*m/z* = 181.04956). The majority of these peaks can be seen when R-Se is analysed together with Na_2S (Figure 4). The remaining peaks, especially those with *m/z*>245, are the result of complex couplings with other R-Se molecules/fragments, and with water or with the solvent (methanol). The low abundance of the protonated molecular peak in ESI-MS spectrum may be an indicator of the readiness of the R-Se compound to react with different compounds, and this reactivity can explain the biological activities found so far for this bioactive compound.

When Na_2S is added to the R-Se solution in 50% methanol/H_2O (Figure 4), the protonated molecular peak of the R-Se (*m/z* = 212.94487) disappears, although the *m/z* = 244.97110 (result of the methanol addition to this peak and also with Se isotopic pattern) can be observed, but with a significant lower abundance than in the spectrum of R-Se alone. It is also possible to observe the peaks of lower *m/z* that were hypothesized above in Figure 2: *m/z* = 135.04414, *m/z* = 149.02, *m/z* = 163.03908 and *m/z* = 181.04958. Besides, new peaks appear. The most relevant of them is the *m/z* = 197.02664, which is the equivalent of the *m/z* = 244.97110 but replacing the Se atom by sulfur (Figure 4 inset). This peak can be formed through the coupling of H_2S (generated *in situ* from Na_2S) with the *m/z* = 163.03908. Finally, two peaks (*m/z* = 266.95303 and *m/z* = 219.00859) with a difference of 48 Da are found, difference that can be attributed to Se-S change, taking into account that the first peak presents the characteristic isotopic pattern of Se. Tentative structures that could explain these two peaks are the polyhydroxy-containing compounds drawn in Figure 4 inset. In any case, the absence of the R-Se protonated molecular peak and the two sulfur-containing peaks (*m/z* = 197.02664, *m/z* = 219.00859) together can be an indicative of an interaction between R-Se and Na_2S.

According to the data obtained, ESI-MS experiments show how this Se-compound, in the electrospray ionization conditions, suffers specific fragmentations (Figure 2) and how it forms complex couplings with the solvent and other R-Se molecules/fragments, indicating that this compound has a high reactivity. This fact could be an indicative of potential interactions of R-Se with the reactive species present in the cell, such as ROS, Reactive Nitrogen Species (RNS) and the sulfur compounds of the redox thiolstat. To prove this hypothetic interaction between R-Se and sulfur species present in cells such as H_2S, we also applied the ESI-MS methodology to a mixture of R-Se and Na_2S. In this second ESI-MS spectrum, it is observed how the peaks of the initial R-Se are practically irrelevant, whereas its fragments peaks are the main peaks. Additionally, new peaks related to couplings of its fragments with the added sulfur atoms start to be observed, proving also the reaction between the two chalcogen compounds.

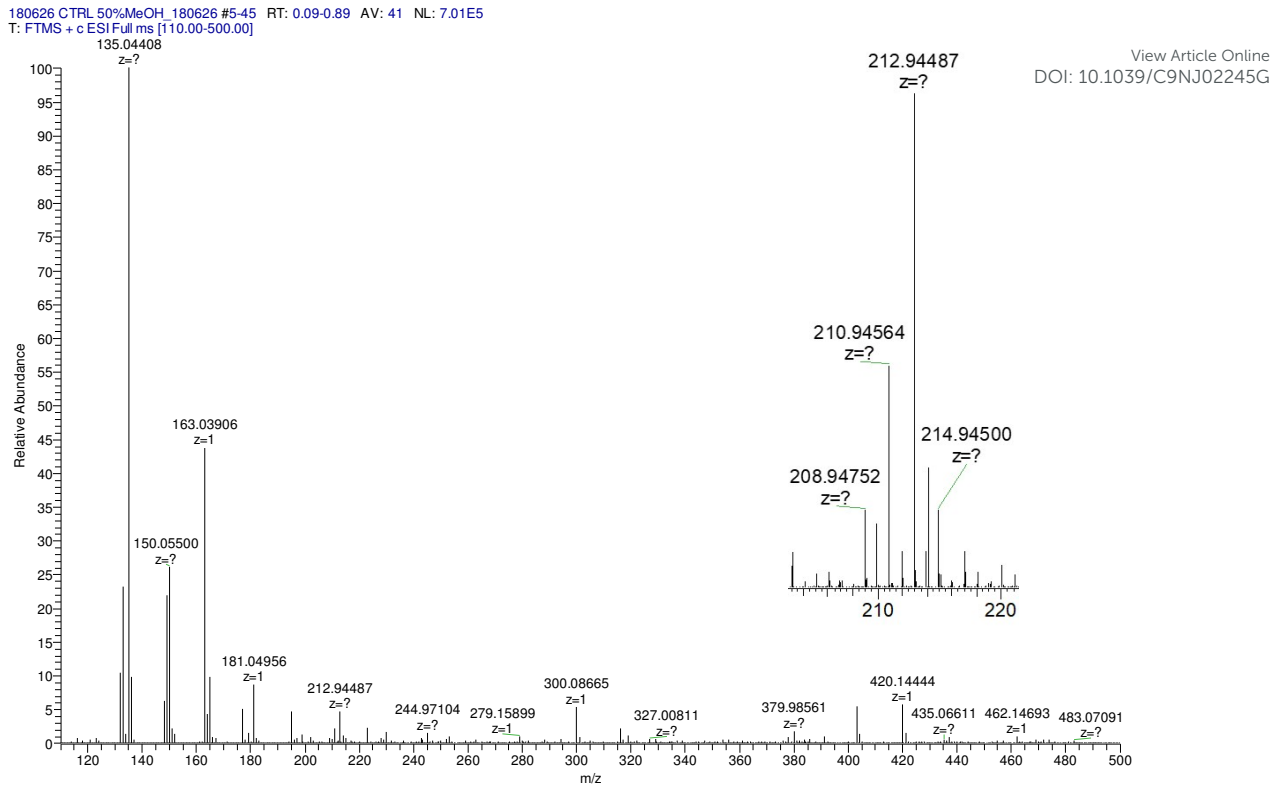

Figure 3: Control R-Se ESI spectrum in 50% methanol/H_2O. Inset: zoom of the protonated molecular peak showing the characteristic isotopic pattern of Se.

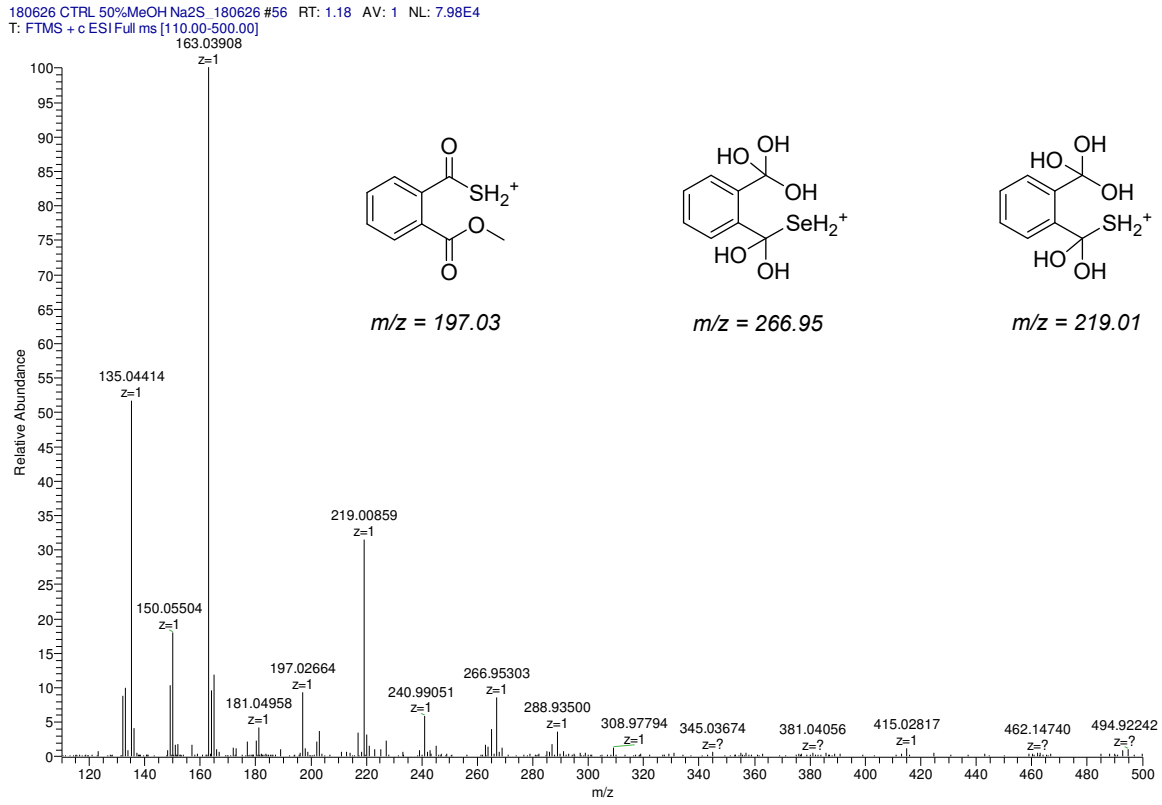

Figure 4: Experimental ESI-MS spectrum of R-Se + Na_2S in 50% methanol/H_2O. Inset: Structures suggested to explain the differential peaks in respect to R-Se ESI-MS spectrum.

Results of the Reduction of •cPTIO by Phthalic-Anhydride Derivatives and H_2S

Since H_2S is endogenously produced in living organisms, we studied the interaction of H_2S with R-Se. We observed that H_2S interacts with R-Se. Since H_2S and Se derivatives were reported to interact with radicals,[54] it was of high interest to reveal whether products of the H_2S/R-Se reaction interact with radicals and how this interaction is unique with comparison to other phthalic-anhydride derivatives. Therefore, we studied the potency of H_2S, R-Se, R-S, R-O and R-OH and the interaction products of H_2S/R-Se, H_2S/R-S, H_2S/R-O and H_2S/R-OH to reduce the •cPTIO radical.

H_2S Potentiates R-Se and R-S (But Not R-O or R-OH) in Reducing •cPTIO. Since H_2S is endogenously produced in organisms and exogenous H_2S donors are being considered to be used in medicine, we have studied interaction of H_2S with anhydride derivatives and the ability of products of this interaction to reduce the •cPTIO radical. H_2S in the presence of R-Se or R-S, but not R-O or R-OH, significantly increased rate and potency of the compounds to reduce •cPTIO (Figures 5A-inset, 5B and 6).

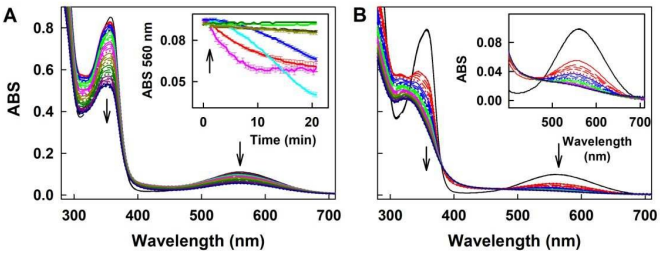

Figure 5. Reduction of •cPTIO by H_2S, R-Se, R-S, RO and R-Se/H_2S mixture. (**A**) Time resolved UV-VIS spectra of 100 µM •cPTIO after addition of 100 µM R-S. Spectra were recorded every 30 s for 20 min. The first spectrum was recorded 15 s after R-S addition. Arrows indicate decrease of ABS at 356 and 560 nm. Inset: Kinetics of changes in absorbance at 560 nm of 100 µM •cPTIO after addition (indicated by arrow) of: 100 µM H_2S (black); 50 and 100 µM R-Se (red and pink); 50 and 100 µM R-S (blue and cyan); 50 and 100 µM R-O (green and dark green) and mixture of 100 µM H_2S with 100 µM R-O (dark yellow). Means ± SEM, n = 2 - 4. (**B**) Time resolved UV-VIS spectra of the interaction of 100 µM •cPTIO with 100 µM H_2S (3 times repeated every 30 s, black) and subsequent addition of 12.5 µM R-Se. Spectra were recorded every 30 s for 20 min, the first spectrum, indicated by the red line, was measured 15 s after addition of R-Se. Inset: details of the time resolved spectra of the •cPTIO/H_2S (100/100 µM/µM) interaction before (black) and after addition of R-Se (12.5 µM, the first spectrum is indicated by the solid red line, which is followed each 30 s by: long dashed red, medium dashed red, short dashed red, dotted red, solid blue line, long dashed blue, medium dashed blue, *etc.*).

Notably, 6.25, 12.5 and 25 µM of R-Se in the presence of 100 µM H_2S had two time-dependent phases of the decreased concentration of 100 µM •cPTIO. The first, it was fast decrease (in ≤ 2 min) followed by the second gradual decrease (Figure 6A). On the other hand, 6.25, 12.5 and 25 µM of R-S decreased •cPTIO in the first phase slower than what was observed when R-Se was employed (≤ 5 min), but later •cPTIO concentration did not decrease significantly (Figure 6C). This indicates that the molecular mechanism of •cPTIO reduction by H_2S/R-Se and H_2S/R-S is different. •cPTIO reduction potency of the H_2S/R-Se mixture was several folds higher than (≥ 5 x) that of H_2S/R-S (Figure 6E). Reduction of •cPTIO strongly depended on H_2S/R-Se molar ratio: it was low at 0.5 and 1 H_2S/R-Se molar ratio but increased significantly at 2 and 4 molar ratios (Figure 6B,F). On the other hand, reduction of •cPTIO gradually increased with H_2S/R-Se molar ratio (Figure 6D,F). The results show that H_2S interacting with R-Se and R-S (but not with R-O or R-OH) forms reactive products, which reduce •cPTIO radical. The order of potency is as follows: H_2S/R-Se > H_2S/R-S >> H_2S/R-O ~ R-OH = 0.

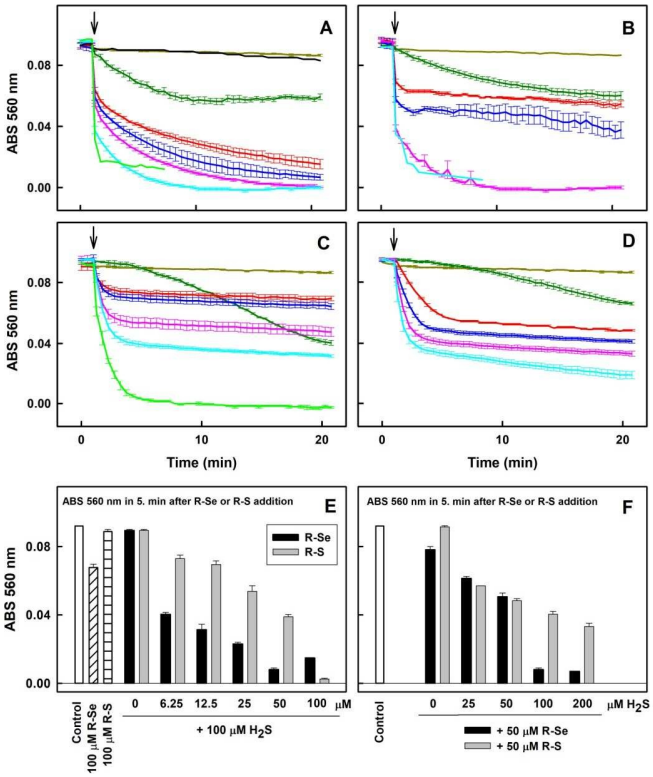

Figure 6. The effect of R-Se and R-S on the kinetics of •cPTIO reduction in the absence and presence of H_2S. (**A)** The effect of R-Se and R-OH on the time-dependent reduction of •cPTIO/H_2S. Kinetics of changes in absorbance at 560 nm of 100 µM •cPTIO after addition (indicated by arrow) of 100 µM R-Se alone (dark green) and compared it to the addition of 0 (dark yellow), 6.25 (red), 12.5 (blue), 25 (pink), 50 (cyan) and 100 µM (green) R-Se to •cPTIO/H_2S (100/100 µM/µM). 50 µM R-OH added to •cPTIO/H_2S (black; 100/100 µM/µM). Data were collected from UV-VIS spectra every 30 s for 20min. **(B)** The effect of H_2S on kinetics of reduction of •cPTIO in the presence of R-Se. Kinetics of changes in absorbance at 560 nm of 100 µM •cPTIO after addition (indicated by arrow) of 100 µM H_2S alone (dark yellow) and after addition of 50 µM R-Se to 0 µM (dark green), 25 µM (red), 50 µM (blue), 100 µM (pink) and 200 µM H_2S (cyan). **(C)** The effect of R-S on the kinetics of •cPTIO reduction in the presence of H_2S. Kinetics of changes in absorbance at 560 nm of 100 µM •cPTIO after addition (indicated by arrow) of 100 µM R-S alone (dark green) and comparison to the addition of 0 (dark yellow), 6.25 (red), 12.5 (blue), 25 (pink), 50 (cyan) and 100 µM (green) R-S to •cPTIO/H_2S (100/100 µM/µM). (**D)** The effect of H_2S on the kinetics of •cPTIO reduction in the presence of R-S. Kinetics of changes in absorbance at 560 nm of 100 µM •cPTIO after addition (indicated by arrow) of 100 µM H_2S alone (dark yellow) and after addition of 50 µM R-S to 0 µM (dark green), 25 µM H_2S (red), 50 µM (blue), 100 µM (pink) and

View Article Online DOI: 10.1039/C9NJ02245G

200 µM H_2S (cyan). **(E)** Comparison of the potency of R-Se and R-S to reduce •cPTIO in the presence of H_2S. Reduction of •cPTIO (100 µM) by R-Se and R-S (100 µM) and reduction of •cPTIO in the presence of H_2S (100 µM) after addition of 0, 6.12, 12.5, 25, 50 and 100 µM R-Se or R-S. The changes in absorbance at 560 nm of 100 µM •cPTIO were taken from (**A,C**) at the 5th min after the addition of compound. **(F)** Comparison of the potency of R-Se and R-S to reduce •cPTIO in the presence of different concentration of H_2S. Reduction of •cPTIO (100 µM) by R-Se and R-S (50 µM) in the presence of 0, 25, 50, 100, 200 µM H_2S. The changes in absorbance at 560 nm of 100 µM •cPTIO were taken from (**B,D**) at the 5th min after the addition of the compound. Means ± SEM, n = 2 - 4.

GSH Potentiates R-Se and R-S (But Not R-O or R-OH) in Reducing •cPTIO. GSH is a tri peptic (glutamate-cysteine-glycine) natural antioxidant, whose intracellular concentrations are in the range of 0.5 to 10 mM.[46,47] Therefore, we studied the effect of GSH on the reducing potency of the phthalic-anhydride derivatives. GSH (100 and 500 µM) did not reduce the •cPTIO (100 µM) radical alone (Figure 7), as observed in our previous study.[42] However, the GSH/R-Se (200/50 and 500/50 µM/ µM) and GSH/R-S (200/50 and 500/50 µM/µM) mixtures significantly reduced •cPTIO (Figure 7). Kinetics of •cPTIO reduction by the mixtures were different for R-Se and R-S. In case of R-S, it was an exponential decay, but in case of R-Se an induction period was observed. The addition of R-O to the •cPTIO/GSH mixture did not cause •cPTIO reduction (Figure 7). The results indicate that the reducing potency of GSH is significantly enhanced upon its interaction with R-Se and R-S. In control experiments, R-O and phthalic acid did not reduce •cPTIO themselves, neither in the presence of 500 µM GSH (Figure 7). This indicates that the presence of Se and S in phthalic anhydride derivatives after interaction with H_2S and GSH is responsible for the reduction of •cPTIO.

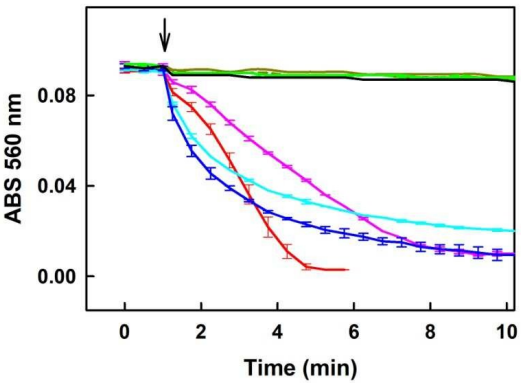

Figure 7. Effect of GSH on •cPTIO reduction kinetics in the presence of R-Se, R-S, R-O and R-OH. Kinetics of the changes in absorbance at 560 nm of 100 µM •cPTIO after addition (indicated by arrow) of 100 (dashed dark-yellow) and 500 µM GSH (solid dark yellow); after addition of 50 µM R-Se to the •cPTIO/GSH (100/200 µM/µM; pink), to the •cPTIO/GSH (100/500 µM/µM; red); after addition of 50 µM R-S to the •cPTIO/GSH (100/200 µM/µM; cyan), to the •cPTIO/GSH (100/500 µM/µM; blue); after addition of 50 µM R-O to the •cPTIO/GSH (100/200 µM/µM; dashed green), to the •cPTIO/GSH (100/500 µM/µM; solid green); after addition of 50 µM R-OH to the •cPTIO/GSH (100/500 µM/µM; black). Means ± SEM, n = 2 - 3.

H_2S and GSH Interacting with Na_2Se-derivatives Reduce •cPTIO. ESI-MS experiments (Figures 3, 4) show that H_2S interacts with R-Se (and its derivatives). We observed that the H_2S/R-Se mixture, but not the H_2S/R-O or H_2S/phthalic acid mixtures, reduced •cPTIO (Figure 6). Based on these data, we suppose that intermediates and/or products of H_2S interaction with Se (released from R-Se) and/or with R-Se derivatives, are responsible for •cPTIO reduction. To confirm this, we studied the interaction of H_2S and GSH with Se derivatives using Na_2Se. UV-VIS spectra of freshly prepared 100 µM Na_2Se changed gradually for 20 min (Figure 8A), which could be an indication of a potential slow unspecific interaction with any of the compounds present in the solution, as the diethylene-triaminepentaacetic acid (DTPA), sodium phosphate, the solvent (water) or most probably with oxygen, which acts as an oxidant. UV-VIS spectra of H_2S/Na_2Se (100/100 µM/µM) also changed gradually for 20 min (Figure 8B). Since the time dependence of the UV-VIS spectra of Na_2Se (Figure 8A) and Na_2Se/H_2S mixture (Figure 8B) were different (marked by arrows), we confirm the interaction of H_2S with Na_2Se derivatives.

The time resolved UV-VIS spectra of •cPTIO/Na_2Se (100/100 µM/µM) shows no •cPTIO reduction by Na_2Se alone, since ABS at 356 nm (marked by arrow) did not decrease over the time (Figure 8C,F), nor ABS at 560 nm (Figure 8C-inset). H_2S (100 µM) or GSH (500 µM) had only minor effects (≤ 7%) on their own in terms of •cPTIO (100 µM) reduction within 20 min. However, addition of freshly prepared Na_2Se (100 µM) to H_2S/•cPTIO (100/100 µM/µM) or GSH/•cPTIO (500/100 µM/µM) mixture reduced •cPTIO (decreased ABS at 356 and 560 nm) in < 1 min (Figure 8D,E,F), indicating a formation of reducing species during the interaction of Na_2Se-derivatives with H_2S and GSH, which reduce the •cPTIO radical. The results support the suggestion that H_2S and GSH significantly potentiated the reducing properties of Se derivatives, which are released from R-Se.

Discussion of the Reduction of •cPTIO by Phthalic-Anhydride Derivatives and H_2S

Regarding the reduction of the •cPTIO radical, R-S and R-Se showed a higher capacity to reduce this radical in comparison with H_2S. But H_2S was most effective in the reduction of the •cPTIO free radical than the phthalic acid and phthalic anhydride. This fact suggests that the mechanism that explains this reduction must be related to a characteristic reaction of R-S and R-Se that is not demonstrated by the R-O or by the R-OH. A potential candidate for the reaction led to this observation could be then the release of sulfide or selenide anions, respectively as the release of O^{2-} is non-existent.H_2S is produced endogenously and exert relevant biological effects and functions. It can be found in tissue cells in non-negligible physiological concentrations that reach even higher than 1 µM.[55] Besides, its local space-time concentration in microenvironments can be even several folds higher. This fact indicates that the H_2S/R-Se interaction may be involved also in

View Article Online
DOI: 10.1039/C9NJ02845C

the biological activities of R-Se. Thus, we have evaluated how it interacts with these chalcogen phthalic derivatives. Results were in line with the previous observations and supported our hypothesis of the S^{2-} and Se^{2-} release: The addition of H_2S to R-S and R-Se potentiated the above mentioned reduction of •cPTIO radical. It is noteworthy the fact that the addition of H_2S promoted the reduction exerted by R-Se more than the one induced by R-S. On the other hand, the addition of H_2S to R-O and R-OH did not exert any effect. Interestingly, the interaction of H_2S with R-Se is dependent on the molar ratio between the Se analogue and H_2S: when R-Se is predominant or when both are equimolar, a low reduction is observed. However, when the molar ratio H_2S/R-Se is 2 to 4, the detected reduction increased significantly. This fact could suggest that a reaction between H_2S and R-Se takes place and that the concentration of the first potentiates this reaction; although the R-Se is also crucial as its replacement by R-S reduced the observed potentiation effect.

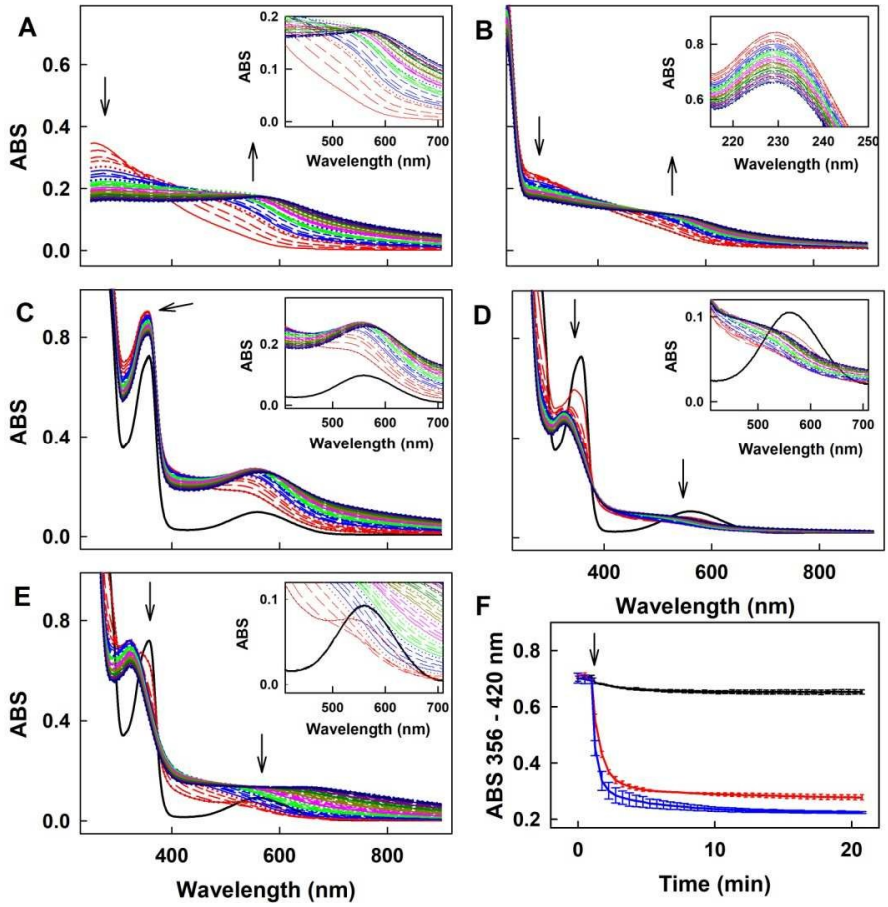

Figure 8. UV-VIS spectra of interaction of Na_2Se with •cPTIO/H_2S and •cPTIO/GSH. (**A**) Time resolved UV-VIS spectra of 100 µM Na_2Se in 100 mM sodium phosphate, 100 µM DTPA, pH 7.4 buffer at 37 °C. Spectra were collected every 30 s for 20 min, the first spectrum was measured 15 s after addition of Na_2Se. Inset are details. The first spectrum is indicated by the solid red line, which is followed each 30 s by: long dashed red, medium dashed red, short dashed red, dotted red, solid blue line, long dashed blue, medium dashed blue, *etc.*; marked by arrows. **(B)** Time resolved UV-VIS spectra of the interaction of 100 µM Na_2Se with 100 µM H_2S. Spectra were collected every 30 s for 20 min, the first spectrum, indicated by the solid red line, was measured 15 s after addition of Na_2Se to H_2S. Inset: details of the time resolved spectra of HS^-, peak at 230 nm. **(C)** Time resolved UV-VIS spectra of the interaction of 100 µM •cPTIO with 100 µM Na_2Se (•cPTIO - 3 times repeated every 30 s, black) and subsequent addition of 100 µM Na_2Se. Spectra were collected every 30 s for 20 min, the first spectrum, indicated by the solid red line, was measured 15 s after addition of Na_2Se. The arrow indicates ABS at 356 nm. Inset: details of the time resolved spectra of the •cPTIO/Na_2Se (100/100 µM/µM) interaction before (black) and after addition of Na_2Se (100 µM). **(D)** Time resolved UV-VIS spectra of the interaction of Na_2Se with •cPTIO/H_2S. Control •cPTIO/H_2S (100/100 µM/µM; 3 times repeated every 30 s, black), and subsequent addition of 100 µM Na_2Se. Spectra were collected every 30 s for 20 min, the first spectrum, indicated by the red line, was measured 15 s after addition of Na_2Se. The arrows indicate decrease of ABS at 356 and 560 nm. Inset: details of the time resolved spectra of the •cPTIO/H_2S (100/100 µM/µM) interaction before (black) and after addition of Na_2Se (100 µM). **(E)** Time resolved UV-VIS spectra of the interaction of Na_2Se with •cPTIO/GSH. Control •cPTIO/GSH (100/500 µM/µM; 3 times repeated every 30 s, black), and subsequent addition of 100 µM Na_2Se. Spectra were collected every 30 s for 20 min, the first spectrum, indicated by the solid red line, was measured 15 s after addition of Na_2Se. The arrows indicate decrease of ABS at 356 and 560 nm. Inset: details of the time resolved spectra of the •cPTIO/GSH (100/500 µM/µM) interaction before (black) and after addition of Na_2Se (100 µM). **(F)** Kinetics of the interaction of Na_2Se (100 µM, marked by arrow) with •cPTIO (100 µM, black), •cPTIO/H_2S (100/100 µM/µM, blue) and •cPTIO/GSH (100/500 µM/µM, red) monitored as changes of ABS at 356 nm with correction to 420 nm; means ± SEM, n = 2 - 3.

View Article Online
DOI: 10.1039/C9NJ02245G

Another sulfur-containing biogenic compound with crucial functions is GSH, which can reach intracellular concentrations in the range 0.5 – 10 mM. Thus, we have also evaluated its interaction with the phthalic anhydride derivatives, as this interaction may be involved in the R-Se biological effects. And effectively, similar results of potentiation of R-Se and R-S ability to reduce the •cPTIO radical were obtained, being then again more significant for R-Se than for R-S. The phthalic anhydride derivatives could interact also with other components of the cellular thiolstat, or even with other different enzymes. For example, they could be activated through different cellular enzymes, such as disulfide reductases and esterases. However, further research needs to be done in future works to confirm this extent. In this study we have selected GSH and H_2S as representative compounds of the sulfur containing components involved in the redox thiolstat. The enhancement of the R-Se activity in respect to the potentiation observed for R-S by the two thiols evaluated (H_2S and GSH) was observed therefore, we tested how H_2S and GSH reduced the •cPTIO radical in the absence of R-Se, finding that in this case there was no interaction. This confirms the key role of R-Se in this interaction, and the requirement of having both Se and S species to have a more effective interaction.

Cleavage of pDNA

We wanted to ascertain whether the products of the H2S/R-Se and/or GSH/R-Se interaction can directly attack pDNA without contribution of other (unknown) biologically important molecules and/or pathways. Briefly, the pDNA cleavage assay can detect any activity that attacks and disrupts the sugar-phosphate backbone of DNA (*e.g.* reactive oxygen species, free radicals *etc.*).

H_2S and GSH Interacting with Phthalic-Anhydride Derivatives Cleave pDNA. To compare the pDNA cleavage activity caused or mediated by the phthalic-anhydride derivatives, increasing concentrations of these compounds were incubated with pDNA *in vitro* and the resulting reaction mixtures were subjected to electrophoretic separation to resolve the individual pDNA forms. R-S, R-O or R-OH had only minor effects on pDNA cleavage. In contrast, R-Se cleaved pDNA in a concentration-dependent manner at concentrations ≥ 50 µM (Figure 9).

Notably, H_2S modulated pDNA cleavage activity of the anhydride derivatives depending on the H_2S/anhydride derivative molar ratio. In the presence of 50 µM of R-Se, the increasing concentrations of H_2S caused the bell-shaped effects with a maximum level being reached at 100/50 and 200/50 µM/µM H_2S/R-Se molar ratios. The effect of 50 µM of R-S, R-O and R-OH was increased with the increasing H_2S concentrations (Figure 10A). In the presence of 100 µM H_2S, pDNA cleavage activity of R-Se was several folds higher with comparison to R-S, R-O or R-OH. Also GSH modulated the pDNA cleavage activity of the anhydride derivatives. In the presence of 50 µM R-Se, increasing concentrations of GSH mediated the bell-shaped effects with a maximum level being seen at 100/50 µM/µM GSH/R-Se molar ratio. In the presence of 50 µM R-S, R-O or R-OH, the increasing concentrations of GSH had no effects on pDNA cleavage (Figure 10B).

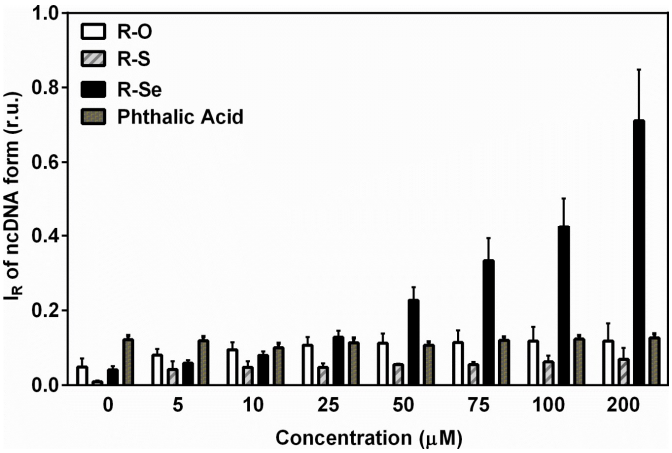

Figure 9. The effect of anhydride-derivatives on pDNA integrity. The increasing concentrations of R-Se, R-S, R-O or phthalic acid were incubated with pDNA for 30 min at 37°C and the resulting pDNA forms were resolved using agarose gel electrophoresis. Mean ± SEM, n = 3.

As we detected relatively similar pDNA cleavage efficiencies at 1:1 and 1:3 molar ratios of R-Se:H_2S, we checked whether there was a difference in kinetics between the two reactions. However, the two reactions displayed the same (linear) time-dependent pDNA cleavage efficiency, suggesting that within a 1:1-1:3 (R-Se:H_2S) molar ratio window, R-Se is a rate-limiting factor in the reaction (Figure 11).

Summing up, we have observed that R-S, R-O and R-OH only exerted a limited pDNA cleavage activity; whereas this activity increased significantly when R-Se was employed in a concentration-dependent manner. Interestingly, the addition of H_2S and GSH modulated strongly this pDNA cleavage action, and showed a bell-shaped effect, suggesting that kinetics may be a rate-limiting factor in this action. In this case, the pDNA cleavage exerted by the remaining phthalic derivatives tested in the presence of H_2S increased in a concentration dependent manner of H_2S, which may be caused by the H_2S-related pDNA cleavage effect. Thus, it is noteworthy that the pDNA cleavage in the absence of H_2S and the bell-shaped modulation in the presence of H_2S and GSH are only observed when R-Se is employed, which underlines the unique redox-modulating properties of R-Se; and which indicates the possibility of the formation of a S-Se intermediate when H_2S interacts with R-Se.

The effect of R-Se, R-S and R-O without and with H_2S to Scavenge the $O_2^{\bullet-}$ Radical or Its Derivatives.

Since we observed that the mixture of H_2S and R-Se or R-S significantly potentiated •cPTIO reduction, it was of interest to study if the mixture can scavenge $O_2^{\bullet-}$ radicals. The EPR spin trap method based on the reaction of $O_2^{\bullet-}$ with BMPO to form the •BMPO-OOH adduct was employed.[56] The $O_2^{\bullet-}$ radical anion solution (prepared by dissolving KO_2 in DMSO) was diluted in phosphate buffer (pH 7.4; 37°C) and trapped by BMPO.

View Article Online
DOI: 10.1039/C9NJ02456C

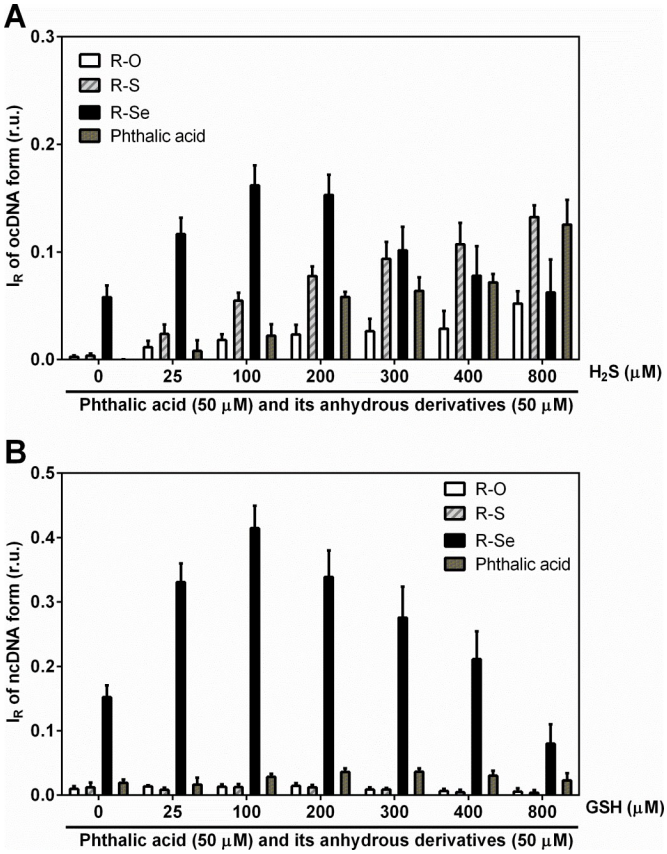

Figure 10. The effect of increasing concentrations of H_2S (A) and GSH (B) on pDNA integrity in the presence of the anhydride-derivatives R-Se, R-S, R-O and R-OH at 50 μM concentrations. Mean ± SEM, n = 3-5.

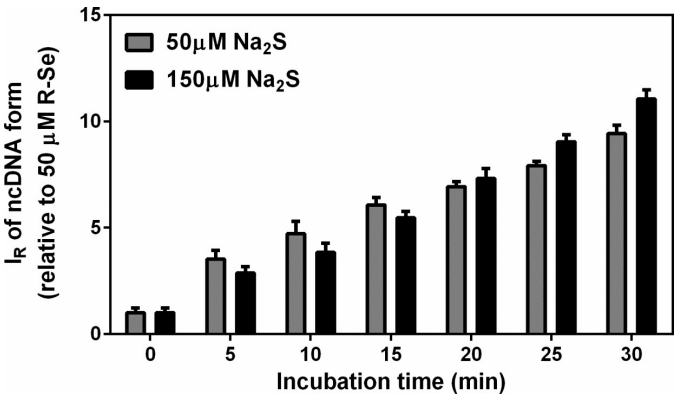

Figure 11. Comparison of time-dependent pDNA cleavage by H_2S/R-Se molar ratios 50/50 and 150/50 μM/μM. The H_2S/R-Se mixture was incubated with pDNA for the given time. I_R of ncDNA was normalized relative to 50 μM R-Se. Mean ± SEM, n = 3.

Under these conditions, the relative intensity of the •BMPO-OOH adduct decreased slowly over the time and was comparable to the values reported under physiological conditions (Figure 12A1-A3).[56] The addition of R-Se or R-O (25 μM) had minor effect on the •BMPO-OOH adduct formation, its concentration or rate of decay (Figure 12B1-B3,D1-D3 and Figure 13A,B). In contrast, R-S (25 μM) significantly decreased the quantity of the •BMPO-adducts (Figure 12C1-C3; Figure 13A,B) and from the decreased ratio of the •BMPO-OOH/•BMPO-adducts (Figure 12C,D), a superposition of at least two radicals, •BMPO-OOH and •BMPO-OH, was recognized. H_2S (50 μM) had similar effects as R-S, however its potency to decrease the quantity of the •BMPO-adducts and ratio of •BMPO-OOH/•BMPO-OH was lower in comparison to R-S (Figure 12E1-E3; Figure 13).

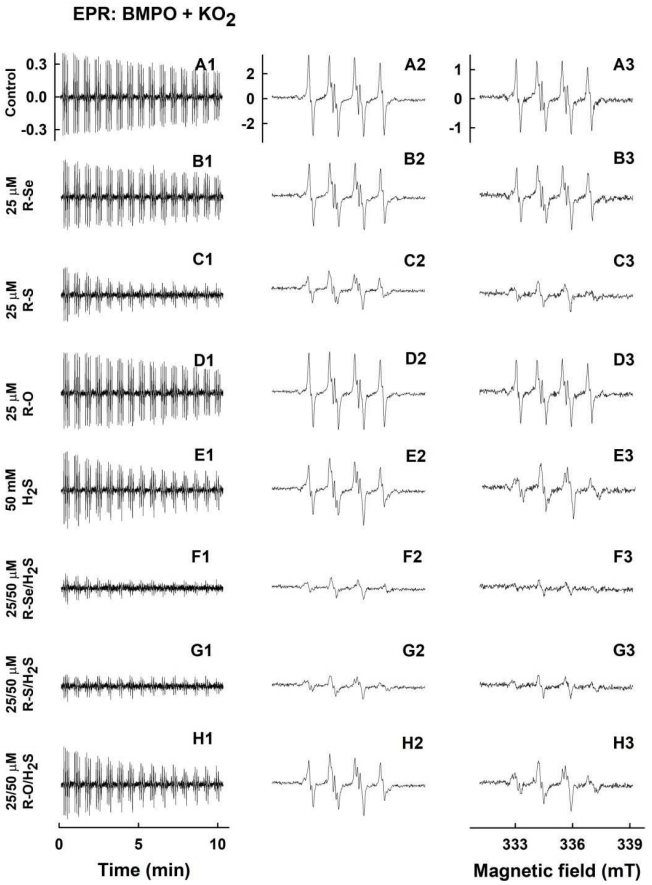

Figure 12. EPR spectra of •BMPO in the presence of $O_2^{\bullet-}$ and modulated by R-Se, R-S and R-O without and with H_2S. Representative EPR spectra of the •BMPO-adducts were monitored in 10% v/v saturated KO_2/DMSO solution in 50 mM sodium phosphate buffer, 0.1 mM DTPA, pH 7.4, 37°C in the presence of the studied species investigated and 20 mM BMPO. Sets of individual EPR spectra of the •BMPO-adducts monitored upon 15 sequential scans, each 42 s (**A1-H1**), starting acquisition 2 min after sample preparation in: control 10% v/v KO_2/DMSO in the buffer (**A1**); the KO_2/DMSO in the presence of 25 μM R-Se (**B1**); 25 μM R-S (**C1**); 25 μM R-O (**D1**); 50 μM H_2S (**E1**); mixture of 25/50 μM/μM R-Se/H_2S (**F1**); mixture of 25/50 μM/μM R-S/H_2S (**G1**) and the mixture of 25/50 μM/μM R-O/H_2S (**H1**). The spectra **A2-H2** show details of the accumulated first ten **A1-H1** spectra. The spectra **A3-H3** show details of the accumulated last five **A1-H1** spectra. The intensities of the time-dependent EPR spectra (**A1-H1**) and detailed spectra (**A2-H2** and **A3-H3**) are comparable, as they were measured under identical EPR settings.

The presence of H_2S (50 μM) in R-Se or R-S (25 μM) solution significantly decreased the quantity of the •BMPO-adducts (Figure 12F1-F3,G1-G3; Figure 13A,B) and significantly decreased the ratio of the •BMPO-OOH/•BMPO-adducts (Figure 13C,D), where a superposition of at least two radicals, •BMPO-OOH and •BMPO-OH, were recognized. On the other hand, a

View Article Online
DOI: 10.1039/C9NJ02245G

mixture of H_2S (50 µM) with R-O (25 µM) caused similar effect as H_2S alone (Figure 12H1-H3; Figure 13). Based on the decreasing quantity of the •BMPO-adducts, we suggest that R-S, H_2S/R-Se and H_2S/R-S scavenge the •BMPO-OOH/OH adducts, which may include a direct scavenging of $O_2^{\bullet-}$ or its derivatives. The decreasing ratio of the •BMPO-OOH/•BMPO-adducts indicates that the compounds cause the decomposition of •BMPO-OOH to •BMPO-OH and scavenge both •BMPO-adducts. However, we cannot exclude the possibility of trapping an unknown radical by BMPO, which decomposed to •BMPO-OH before measurement of the sample. Our data suggest that R-S, H_2S/R-Se and H_2S/R-S have high potency to scavenge different radicals.

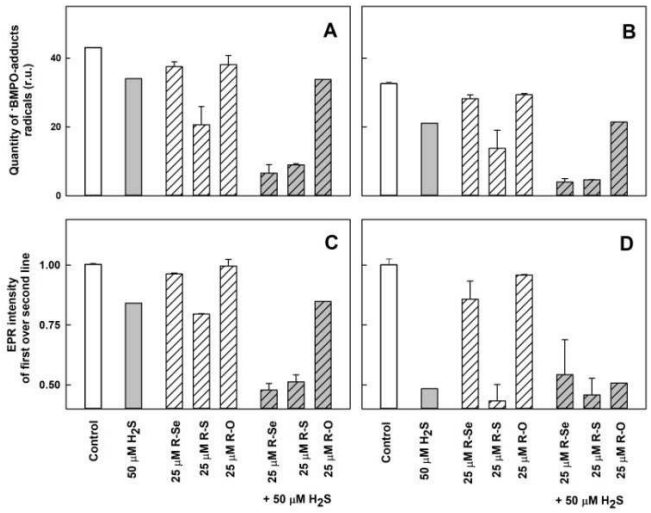

Figure 13. The effects of compounds on the •BMPO-adducts radicals. The effects of compounds (25 µM) and their mixture with H_2S (50 µM) on quantity of the •BMPO-adducts radicals (double integral of EPR spectra from Figure 12) in the presence of 10% v/v saturated KO_2/DMSO solution. Average radical quantity during 2-9 (**A**, from Figure 12A2-H2) and 10-13 (**B**, from Figure 12A3-H3) min after sample preparation. The effects of compounds (25 µM) and their mixture with H_2S (50 µM) on EPR intensity of the ration of the first over the second line spectra of the •BMPO-adducts radicals (data from Figure 12). Average ration during 2-9 (**C**, from Figure 12A2-H2) and 10-13 (**D**, from Figure 12A3-H3) min after sample preparation. Buffer: 50 mM sodium phosphate, 0.1 mM DTPA, pH 7.4, 37°C. Means ± SEM, n=2

To summarize this section, taking into account the ability of the phthalic derivatives to reduce the •cPTIO radical, we have studied also how these derivatives interact with $O_2^{\bullet-}$ observing how they interfere with the formation of the •BMPO-OOH adduct in the presence of KO_2 and BMPO. In this experiment, R-Se and R-O showed a minor interaction with $O_2^{\bullet-}$ radical, whereas R-S significantly decreased the formation of the •BMPO-OOH adduct. Interestingly, the addition of H_2S to R-Se and to R-S significantly enhances their capacity to decrease the formation of the •BMPO-OOH adduct, again highlighting the enhanced activity of the products of the interaction between H_2S and R-Se: The presence of both Se and S atoms seems to be crucial for all these activities.

Final discussion

At the sight of the results presented herein, we suggest that the products of H_2S or GSH interaction with R-Se, having free radical scavenging and pDNA cleavage activities, can also affect intracellular molecules other than DNA. Based on the well-known consequences of oxidative stress, protein oxidation is also highly expected. We are aware of the fact that much more effects should be examined to obtain a more complete picture on action of products of H_2S or GSH interaction with R-Se and our intention is to present these promising initial results.

In summary, the results confirm our initial hypothesis: the selenoanhydride (R-Se) can act as a H_2Se donor, serving as a prodrug that enables the internalisation of the selenium in the cells, and the subsequent release of H_2Se and ionic species of Se inside the cell. Besides, we have proved that H_2S and GSH interact with R-Se, and that the intermediates and/or products of this interaction have significant properties to reduce (scavenge) the •cPTIO and superoxide ($O_2^{\bullet-}$) radicals or its derivatives and to cleave pDNA. The observed antioxidant (reducing) properties of intermediates and/or products of the H_2S/R-Se and GSH/R-Se interaction to reduce •cPTIO, scavenge $O_2^{\bullet-}$ and decompose •BMPO-OOH to •BMPO-OH, indicate that they may modulate redox properties and free radical signalling. However, qualifying the significance of these observations is a challenge for future research

Experimental

Chemical Synthesis of the Anhydride-derivatives

R-Se and R-S (Figure 1) were synthetized according to a procedure based in the one previously described in literature[49], with minor modifications, whereas R-O was commercially available. Briefly, a suspension of grey selenium (for R-Se) or elemental sulfur (for R-S) in water-free tetrahydrofuran is reduced by a drop wise addition of lithium aluminium hydride. Once completed the reaction (visible by the ceasing of the generation of molecular hydrogen), phthaloyl chloride is added to the reaction and left reacting till the end of the reaction (usually 1 h). Then, solution is filtered to eliminate the metallic salts generated during the process, and over the filtrate, a 10 mL of concentrated sulfuric acid are added drop wise. Mixture is left reacting and the solid formed is filtered and washed with chloroform. The product isolated from the organic fraction is recrystallized in hexane.

The structure of the compounds R-Se and R-S was confirmed by NMR-^{1}H, and their purity, by LC-MS. Spectra are provided in Supplementary Material and they are in accordance with bibliography. The purity of both compounds was 100%, according LC-MS (see data in Supplementary), so both derivatives were suitable for biological evaluation as they accomplish the 95% of purity considered as the minimum threshold purity value required for biological assays. The chemical reactions of this synthetic procedure were shown in Figure 1. It is quite interesting to see how the reaction normally used to get the oxygen anhydrides (dehydration of the phthalic

View Article Online
DOI: 10.1039/C9NJ03245G

acid) also serves to synthesize the sulfur and selenium anhydrides analogues. What is more, it is noteworthy to point the selectivity of the formation of the respective thio- and selenoanhydride when an oxygen atom is bound to the second carbonyl of the intermediate chalcogen phthalate.

In a previous work in a PhD dissertation[57], to learn more about the reactivity of different phthalic derivatives to form the phthalic selenoanhydride (R-Se) following this procedure, a synthetic study was performed. R-Se was synthesized according to the procedure mentioned above departing from phthaloyl chloride and using lithium aluminium hydride for the reaction. The yield before recrystallization in this case was a 94%. When the reaction was carried using water as solvent and employing sodium borohydride as reducing agent, yield before recrystallization was 47%. Reaction could also use different phthalic derivatives as substrates (always employing lithium aluminium hydride), in this case with different yields. We explored phthalic anhydride and N-hydroxyphthalimide, achieving yields of 16% and 62%, respectively. Interestingly (unpublished results), phthalimide did not render the R-Se after the dehydration with sulfuric acid. It seems that a selenazine is formed instead of the selenoanhydride, obtaining the 1*H*-benzo[*d*][1,2]selenazine-1,4(3*H*)-dione. Unfortunately, this compound could not be obtained with a satisfactory purity and more research needs to be done to isolate and characterize this compound.

For pDNA cleavage assay, the anhydride-derivatives were dissolved in ultrapure deionized water at 1 mM final concentration by vortexing and 1 min water bath sonication, subsequently aliquoted and stored at -80°C before their use. For UV-VIS, EPR and ESI studies, the anhydride-derivatives were dissolved in anhydrous DMSO at 50 mM concentration, aliquoted and stored at -80°C before being used.

ESI-MS Measurement

Saturated R-Se was prepared in 50% methanol/H_2O, vortexed for 2-3 min, sonicated in water bath for 1-2 min and centrifuged for 2 min. The sample without and with 7 mM Na_2S (~ 9 pH) was incubated for 1 min at 37°C and 55 µl of the supernatant was used to measure ESI-MS spectra (Orbitrap Elite, ThermoScientific).

Chemicals for UV-VIS and EPR measurements

The studied compounds, R-Se, R-S and R-O in DMSO (50 mM) were used after thawing. The spin trap 5-*tert*-butoxycarbonyl-5-methyl-1-pyrroline-*N*-oxide (BMPO, 100 mM, ENZO Life Sciences AG, Switzerland) was prepared in deionized H_2O, stored at -80°C and used after thawing. The radical 2-(4-carboxyphenyl)-4,4,5,5-tetramethylimidazoline-1-oxyl-3-oxide (•cPTIO, 10 mM, Cayman 81540 or Sigma C221) in deionized H_2O was stored at -20°C for several weeks. Na_2S as a source of H_2S (100 mM; SB01, DoJindo, Japan) was prepared in deionized H_2O, stored at -80°C and used after thawing. Na_2S dissociates in solution and reacts with H^+ to yield H_2S, HS^- and a trace of S^{2-}. We use the term H_2S to encompass the total mixture of H_2S, HS^- and S^{2-}. To Na_2Se powder (Alfa Aesar, 36187, stored under argon) H_2O was added, and in 10 s aliquot of the stock Na_2Se solution (10 mM) was added to UV-VIS cuvette containing studied compounds. 100 mM sodium phosphate buffer supplemented with 100 µM DTPA, pH 7.4, 37°C, was employed for UV-VIS experiments. 50 and 25 mM sodium phosphate buffer, supplemented with 100 and 50 µM DTPA (diethylenetriaminepentaacetic acid), pH 7.4, 37°C was used for electron paramagnetic resonance (EPR) studies.

UV-VIS of •cPTIO

To basic 900 - 990 µl solution of 100 mM sodium phosphate, 100 µM DTPA buffer (pH 7.4, 37°C) the final concentrations of 100 µM •cPTIO and Na_2S was added and the UV-VIS spectra (900 – 190 nm) were recorded 3 x 30 s. Studied compounds, R-Se, R-S and R-O (50 mM in DMSO) firstly dissolved in 50 µl buffer and vortexed for 3 s were added and the spectra were recorded every 30 s for 20 min using a Shimadzu 1800 (Kyoto, Japan) spectrometer at 37°C (blank was H_2O). For our study, the •cPTIO extinction coefficient at 560 nm of 920 M^{-1} cm^{-1} was used. Scavenging of the •cPTIO radical by Na_2S (H_2S) or GSH and its mixture with studied compounds R-Se, R-S and R-O was determined as a decrease of absorbance at 356 and 560 nm (absorption maximum of •cPTIO) after subtraction of baseline absorbance, which were determined at 730 or 420 nm, respectively.[42]

Plasmid DNA Cleavage

The pDNA cleavage assay, which detects a disruption of the sugar-phosphate backbone of DNA, was used to study if the products of the H_2S/R-Se and/or GSH/R-Se interaction can directly attack pDNA. In this assay, even a single hit is trapped, as it converts the circular supercoiled DNA molecule into its nicked relaxed circular form. These two forms display distinct mobility in agarose gels, and therefore they can easily be distinguished and quantified.

The pBR322 vector (4.361 kb, New England Biolabs, N3033L) was used in pDNA cleavage assay. In this assay, all samples contained 200 ng of pDNA in a final volume of 20 µl of buffer composed of 25 mM sodium phosphate and 50 µM DTPA (pH 7.4). Three different assay conditions were used: i) pDNA *per se* (control), ii) pDNA + phthalic-anhydride derivatives, and iii) pDNA + anhydride-derivative + Na_2S or GSH. The resulting mixtures were incubated for 30 min at 37°C. Afterwards, the reaction mixtures were subjected to 0.6% agarose gel electrophoresis. The samples were electrophoresed in TBE buffer (89 mM Tris, 89 mM boric acid, 2 mM EDTA, pH 8.0) at 5.5 V/cm for 2 h. The gel was stained with Gel Red™Nucleic Acid Gel Stain. Finally, the gels were photographed using a UV transilluminator. To quantify the pDNA cleavage efficiency, the integrated densities of two identified pBR322 forms (a supercoiled and a nicked circular form) in each lane were quantified using Total Lab TL100 image analysis software (Nonlinear Dynamic Ltd., USA).

EPR of •BMPO-adducts

To study the ability of R-Se, R-S and R-O without and with H_2S to scavenge the $O_2^{\bullet-}$ radical produced in DMSO/KO_2 solution,

View Article Online DOI: 10.1039/C9NJ02245G

sample preparation and EPR measurements were conducted in accordance with previously reported protocols.[42] The solution (final concentrations) of BMPO (20 mM), DTPA (100 μM) in sodium phosphate buffer (50 mM, pH 7.4) was incubated for 1 min at 37°C. An aliquot of the compounds studied was added, followed by the addition of Na_2S in 3 s and saturated KO_2/DMSO solution (10% v/v DMSO/final buffer) 3 s later. The sample was mixed for 5 s and the first EPR spectrum was recorded 2 min after the addition of KO_2/DMSO solution at 37°C. The sets of individual EPR spectra of the •BMPO spin-adducts were recorded as 15 sequential scans, each 42 s, with a total time of 11 min. Each experiment was repeated at least twice. EPR spectra of the •BMPO spin-adducts were measured on a Bruker EMX spectrometer, X-band ~9.4 GHz, 335.15 mT central field, 8 mT scan range, 10 mW microwave power, 0.1 mT modulation amplitude, 42 s sweep time, 20.48 ms time constant, and 20.48 ms conversion time at 37°C.

The relative quantity of the •BMPO-adducts radicals was calculated as double integral of EPR spectra. Since EPR spectra were mostly low intensity, which did not permit spectral simulation, to quantify relative ratio of the •BMPO-OOH/•BMPO-adducts, the ratio of EPR intensity of the first line over the second line was used. The ratio is ~ 1 at ~ 100 % of •BMPO-OOH (Figure 12A2) and ~ 0.5 at ~ 0 % of •BMPO-OOH.[42] The lower ratio (lower than 1) indicates higher concentration of other •BMPO-adducts, in which mostly •BMPO-OH radicals are present.

Conclusions

Understanding of the molecular mechanism of biological effects of phthalic-anhydride derivatives could lead to development of more efficient drugs for treatment of cancer and ROS related diseases. To achieve this, we found, that phthalic-anhydride derivatives, R-Se, R-S, R-O and R-OH (≤ 50 μM) on their own have minor potency to reduce/scavenge radicals or cleave pDNA. However, the potency of R-Se and R-S, but not R-O or R-OH, significantly increased after interacting with H_2S and GSH.

Our *in-vitro* data revealed unique properties of the H_2S/R-Se, GSH/R-Se and H_2S/R-S mixtures to reduce the •cPTIO and superoxide radicals. The unique potency of the H_2S/R-Se mixture to cleave pDNA has the bell-shaped dependence on H_2S and GSH concentrations, whereas potency of H_2S/R-S increased linearly with H_2S, but did not increase with GSH concentration. The results underline that the interactions of R-Se and R-S with H_2S and GSH enhanced significantly the different activities monitored, thus indicating that the intermediates and/or the products of the interaction of R-Se and R-S with endogenous H_2S and GSH have significant antioxidant properties and that they can damage DNA. These findings may contribute to understand more-in-depth the unique biological effects reported so far for R-Se and R-S. Besides, these findings open a new so far unexplored approach to study the action of the Se-containing compounds. These experiments, for example, can be applied to the different selenium species that have been used until now in supplementation, to ascertain which ones have more ability to interact with GSH and H_2S. This is of crucial importance, as it would enable detecting new compounds that could behave as Se-based redox modulators in a potential Se supplementation. An example would be the phthalic selenoanhydride (R-Se) reported in this work, which maintains the capacity of sodium selenite to react with key components of the redox thiolstat (as GSH and H_2S) and simultaneously, according to previous works, shows a lower toxicity against non-tumour cells.

Conflicts of interest

There are no conflicts to declare.

Author Contributions: Conceptualization, E.D-A., C.J., M.C., and K.O.; Methodology, K.O., M.C., and V.B.; Validation, K.O., M.C., V.B., A.M., M.G., and E.D.-A.; Formal Analysis, A.M., and K.O., Investigation, A.M., M.G., A.K., V.B., L.K., P.B., M.C., K.O., and E. D.-A.; Resources, A.K., C.J., and E.D.-A.; Writing-Original Draft Preparation, K.O., M.C., and E.D.-A.: Visualization, K.O., A.M., M.G., and E.D.-A.; Supervision, K.O., C.J., M.C., and E.D.-A.; Project Administration, K.O., C.J., M.C., and E.D.-A.; Funding acquisition, K.O.

Acknowledgements

This research was funded by the Slovak Research & Development Agency, grant numbers APVV-15-0371, 14-0783, 15-0565 and 17-0384 and the Scientific Grant Agency of the Slovak Republic, grant numbers VEGA 1/0041/15, 1/0026/18, 2/0146/16, and 2/0014/17. The authors would also like to acknowledge the financial support of the Agencia Estatal Consejo Superior de Investigaciones Científicas (Spain, project 201780I027) and of the University of Saarland. We also thank, Prof. Dr. Anna K. H. Hirsch and Dr. Eleonora Diamanti from Helmholtz Institute for Pharmaceutical Research in Saarland (HIPS) for helping with MS spectra measurements.

Notes and references

1 S. J. Fairweather-Tait and K. Cashman, in *Nutrition for the Primary Care Provider. World Rev Nutr Diet,* vol 111, ed. D.M. Bier, J. Mann, D. H. Alpers, H. H. E. Vorster and M. J. Gibney, Karger AG, Basel, Switzerland, 2015, Ch 8, pp. 45-52.;
2 S. Li, T. Xiao and B. Zheng, *Sci Total Environ*, 2012, **421-422**, 31-40.
3 S. Stranges, J. R. Marshall, R. Natarajan, R. P. Donahue, M. Trevisan, G. F. Combs, F. P. Cappuccio, A. Ceriello and M. E. Reid, *Ann Intern Med*, 2007, **147,** 217-223.
4 D. L. Hatfield, M. H. Yoo, B. A. Carlson and V. N. Gladyshev, *Biochim Biophys Acta Gen Subj*, 2009, **1790,** 1541-1545.
5 J. C. Avery and P. R. Hoffmann, *Nutrients*, 2018, **10**, 1203.
6 N. Shang, X. Wang, Q. Shu, H. Wang and L. Zhao, *J Nanosci Nanotechnol*, 2019, **19**, 1875-1888.
7 K. M. Peters, B. A. Carlson, V. N. Gladyshev, and P. A. Tsuji, *Free Radic Biol Med*, 2018, **127**, 14-25.
8 V. Gandin, P. Khalkar, J. Braude and A. P. Fernandes, *Free Radic Biol Med*, 2018, **127**, 80-97.

9 M. Bodnar, M. Szczyglowska, P. Konieczka, J. Namiesnik. *Crit Rev Food Sci Nutr,* 2016, **56**, 36-55.
10 A. Tarze, M. Dauplais, I. Grigoras, M. Lazard, N. T. Ha Duong, F. Barbier, S. Blanquet, P. Plateau, *JBC*, 2007, **282**, 8759–8767.
11 A. P. Fernandes and V. Gandin, *Biochim Biophys Acta Gen Subj*, 2015, **1850**, 1642-1660.
12 J. J. An, K. J. Shi, W. Wei, F. Y. Hua, Y. L. Ci, Q. Jiang, F. Li, P. Wu, K. Y. Hui, Y. Yang and C. M. Xu, *Cell Death Dis.* **2013,** 4, e973.
13 G. Nilsonne, X. Sun, C. Nyström, A.K. Rundlöf, A. Potamitou Fernandes, M. Björnstedt and K. Dobra, *Free Radic Biol Med*, 2006. **41**, 874-885.
14 J. Brozmanová, D. Mániková, V. Vlčková and M. Chovanec, *Arch Toxicol*, 2010, **84**, 919-938.
15 E. Jablonska and M. Vinceti, *J Environ Sci Health Part C Environ Carcinog Ecotoxicol Rev*, 2015, **33**, 328-368.
16 H. J. Reich and R. J. Hondal, *ACS Chem Biol*, 2016, **11**, 821-841.
17 R. Mousa, R. Notis Dardashti and N. Metanis, N. *Angew Chem Int Ed*, 2017, **56**, 15818-15827.
18 C. Jacob, G. I. Giles, N. M. Giles and H. Sies, H. *Angew Chem Int Ed*, 2003, **42**, 4742-4758.
19 L. Sancineto, M. Palomba, L. Bagnoli, F. Marini, C. Santi. *Curr Org Chem*, 2016, **20**, 122-135.
20 D. Bartolini, L. Sancineto, A. Fabro de Bem, K. D. Tew, C. Santi, R. Radi, P. Toquato and F. Galli, In *Advances in Cancer Research, Volume 136*, ed. K. D. Tew and F. Galli. Academic Press Inc., Cambridge, United States, 2017, Ch. 10, pp 259-302.
21 C. Santi, C. Tomassini, L. Sancineto. *Chimia (Aarau)*, 2017, **71**, 592-595.
22 M. Álvarez-Pérez, W. Ali, M. A. Marć, J. Handzlik and E. Domínguez-Álvarez, *Molecules*, 2018, **23**, 628.
23 W. Ali, M. Álvarez-Pérez, M. A. Marć, N. Salardón-Jiménez, J. Handzlik and E. Domínguez-Álvarez, *Curr Pharmacol Rep*, 2018, **4**, 468-481.
24 S. Misra, M. Boylan, A. Selvam, J. E. Spallholz and M. Björnstedt, *Nutrients*, 2015, **7**, 3536-3556.
25 C.M. Weekley and H. H. Harris, *Chem Soc Rev*, 2013, **42**, 8870-8894.
26 R. Terazawa, D. R. Garud, N. Hamada, Y. Fujita, T. Itoh, Y. Nozawa, K. Nakane, T. Deguchi, M. Koketsu and M. Ito, *Bioorg Med Chem*, 2010, **18**, 7001-7008.
27 B. Romano, D. Plano, I. Encío, J. A. Palop and C. Sanmartín. *Bioorg Med Chem*, 2015, **23**, 1716-1727.
28 Y. Zakharia, A. Bhattacharya and Y. M. Rustum, *Oncotarget*, 2018, **9**, 10765-10783
29 C. Santi, C. Tidei, C. C. Scalera, M. Piroddi, and F. Galli. *Curr Chem Biol*, 2013, **7**, 25-36.
30 D. Bartolini, M. Piroddi, C. Tidei, S. Giovagnoli, D. Pietrella, Y. Manevich, K. D. Tew, D. Giustarini, R. Rossi, D. M. Townsend, C. Santi and F. Galli. *Free Radic Biol Med*, 2015, **78**, 56-65.
31 M. M. Rahman, R. A. Uson-Lopez, M. T. Sikder, G. Tan, T. Hosokawa, T. Saito and M. Kurasaki, *Chemosphere*, 2018, **196**, 453-466.
32 M. Mix, N. Ramnath, J. Gomez, C. De Groot, S. Rajan, S. Dibaj, W. Tan, Y. Rustum, M. B. Jameson and A. K. Singh, *World J Clin Oncol*, 2015, **6**, 156-165.
33 D. Mániková, L. M. Letavayová, D. Vlasáková, P. Košík, E. C. Estevam, M. J. Nasim, M. Gruhlke, A. Slusarenko, T. Burkholz, C. Jacob and M. Chovanec, *Molecules*, 2014, **19**, 12258-12279.
34 C. Sanmartín, D. Plano, M. Font, and J. A. Palop, *Curr Cancer Drug Targets*, 2011, **11**, 496-523.
35 R. Wang, *Physiol Rev*, 2012, **92**, 791-896.
36 C. Szabo and A. Papapetropoulos, *Pharmacol Rev*, 2017, **69**, 497-564.
37 H. Kimura, *Antioxid Redox Signal*, 2015, **22**, 362-376.
38 M. Whiteman, J. S. Armstrong, S. H. Chu, S. Jia-Ling, B. S. Wong, N. S. Cheung, B. Halliwell and P. K. Moore, *J Neurochem*, 2004, **90**, 765-768.
39 M. Whiteman, N. S. Cheung, Y. Z. Zhu, S. H. Chu, J. L. Siau, B. S. Wong, J. S. Armstrong and P. K. Moore, *Biochem Biophys Res Commun*, 2005, **326**, 794-798.
40 A. Staško, V. Brezová, M. Zalibera, S. Biskupič, and K. Ondriaš, *Free Radic Res*, 2009, **43**, 581-593.
41 B. Olas, *Chem-Biol Interact*, 2014, **217**, 46-56.
42 A. Misak, M. Grman, Z. Bacova, I. Rezuchova, S. Hudecova, E. Ondriasova, O. Krizanova, V. Brezova, M. Chovanec and K. Ondrias, *Nitric Oxide*, 2018, **76**, 136-151.
43 C. Szabo, C. Coletta, C. Chao, K. Módis, B. Szczesny, A. Papapetropoulos and M. R. Hellmich. Proc Natl Acad Sci U S A, 2013, **110**, 12474-12479
44 D. Wu, W. Si, M. Wang, S. Lv, A. Ji and Y. Li, *Nitric Oxide*, 2015, **50**, 38-45.
45 J. Jr. Breza, A. Soltysova, S.; Hudecova, A. Penesova, I. Szadvari, P. Babula, B. Chovancova, L. Lencesova, O. Pos, J. Breza, K. Ondrias, and O. Krizanova, *BMC Cancer*, 2018, **18**, 591.
46 V. I. Lushchak, *J Amino Acids*, 2012, **2012**, 736837.
47 C. Gaucher, A. Boudier, J. Bonetti, I. Clarot, P. Leroy and M. Parent, *Antioxidants*, 2018, **7**, 62.
48 A. Kharma, M. Grman, A. Misak, E. Domínguez-Álvarez, M.J. Nasim, K. Ondrias, M. Chovanec, C. Jacob. *Molecules*, 2019, **24**, 1359.
49 E. Domínguez-Álvarez, D. Plano, M. Font, A. Calvo, C. Prior, C. Jacob, J.A. Palop and C. Sanmartín, *Eur J Med Chem*, 2014, **73**, 153-166.
50 M. J. Nasim, W. Ali, E. Domínguez-Álvarez, E. N. da Silva Júnior, R. S. Z. Saleem and C. Jacob, in *Organoselenium Compounds in Biology and Medicine: Synthesis, Biological and Therapeutic Treatments*, ed. V. K. Jain and K. I. Priyadarsini, The Royal Society of Chemistry, Croydon, United Kingdom, 2018, Ch. 10, pp 277-302.
51 M. Gajdács, G. Spengler, C. Sanmartín. M. A. Marć, J. Handzlik and E. Domínguez-Álvarez, *Bioorg Med Chem Lett*, 2017, **27**, 797-802.
52 E. Domínguez-Álvarez, M. Gajdács, G. Spengler, J. A. Palop, M. A. Marć, K. Kieć-Kononowicz, L. Amaral, J. Molnár, C. Jacob, J. Handzlik and C. Sanmartín, *Bioorg Med Chem Lett*, 2016, **26**, 2821-2824.
53 M. M. Cortese-Krott, G. G. C. Kuhnle, A. Dyson, B. O. Fernandez, M. Grman, J. F. DuMond, M. P. Barrow, G. McLeod, H. Nakagawa, K. Ondrias, P. Nagy, S. B. King, J. E. Saavedra, L. K. Keefer, M. Singer, M. Kelm, A. R. Butler and M. Feelisch, *Proc Natl Acad Sci U S A*, 2015, **112**, E4651-E4660.
54 M. T. Zimmerman, C. A. Bayse, R. R. Ramoutar and J. L. Brumaghim, *J Inorg Biochem*, 2015, **145**, 30-40.
55 Y. H. Liu, M. Lu, L. F. Hu, P. T. H. Wong, G. D. Webb and J. S. Bian, *Antioxid Redox Signal*, 2012, **17**, 141-185.
56 H. Zhao, J. Joseph, H. Zhang, H. Karoui and B. Kalyanaraman. *Free Radic Biol Med*, 2001, **31**, 599-606.
57 Domínguez-Álvarez E. PhD Dissertation. University of Navarra (Spain), 2012.

View Article Online
DOI: 10.1039/C9NJ02245G

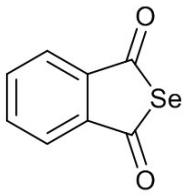

Previously reported biological activities

- ✓ Anticancer agent
- ✓ Antimicrobial
- ✓ Apoptotic inducer
- ✓ Efflux pump inhibitor
- ✓ MDR-reversing agent

Effects of phthalic selenoanhydride (R-Se)

- ✓ Reduces •cPTIO radical. ↑ reduction that its S isostere
- ✓ ↑ reduction observed in presence of H_2S or GSH
- ✓ Cleaves pDNA in a concentration dependent manner at concentrations ≥ 50 µM
- ✓ The presence of H_2S ↑ the pDNA cleavage of R-Se
- ✓ Scavenges $O_2^{\bullet-}$ radical in presence of H_2S

Suggested mechanism of action

R-Se releases H_2Se, anionic forms of selenium or elemental selenium nanoparticles. These released compounds are behind the observed activities